

Supplementary Information for “Doping-induced magnetism and magnetoelectric coupling in one-dimensional NbOCl₃ and NbOBr₃”

Ruiman He, Pengyu Liu, Bing Wang, Jinbo Fan*, and Chang Liu*

*Institute for Computational Materials Science, Joint Center for Theoretical Physics (JCTP),
School of Physics and Electronics, Henan University, Kaifeng, 475004, China*

Corresponding author: jinbofan1988@126.com; cliu@vip.henu.edu.cn

Table S1. Total magnetic moments of different elements in the top and bottom cell as well as their moment differences for n-L nanochain of NbOCl₃, electing the doping concentration of $2.9 \times 10^{14}/\text{cm}^2$ and $\Delta\mu = \mu_{\text{top}} - \mu_{\text{bot}}$.

	2-L	3-L	4-L	5-L	6-L
Nb_{top}	0.696	0.806	0.95	1.006	1.036
Nb_{bot}	0.242	0.294	0.304	0.344	0.354
$\Delta\mu_{Nb}$	0.454	0.512	0.646	0.662	0.682
Cl_{top}	0.074	0.072	0.09	0.09	0.09
Cl_{bot}	0.008	0.014	0.004	0.006	0.006
$\Delta\mu_{Cl}$	0.066	0.058	0.086	0.084	0.084
O_{top}	-0.032	-0.04	-0.044	-0.048	-0.05
O_{bot}	-0.016	-0.018	-0.022	-0.024	-0.024
$\Delta\mu_O$	-0.016	-0.022	-0.022	-0.024	-0.026

Table S2. Total magnetic moments of different elements in the top and bottom cell as well as their moment differences for n-L nanochain of NbOBr₃, electing the doping concentration of $2.9 \times 10^{14}/\text{cm}^2$ and $\Delta\mu = \mu_{\text{top}} - \mu_{\text{bot}}$.

	2-L	3-L	4-L	5-L	6-L
Nb_{top}	0.76	0.794	1.068	1.04	1.11
Nb_{bot}	0.264	0.29	0.232	0.288	0.326
$\Delta\mu_{Nb}$	0.496	0.504	0.836	0.752	0.784
Br_{top}	0.034	0.024	0.098	0.098	0.099
Br_{bot}	0.01	0.014	-0.008	0	0.002
$\Delta\mu_{Br}$	0.024	0.01	0.106	0.098	0.097
O_{top}	-0.048	-0.054	-0.052	-0.052	-0.056
O_{bot}	-0.016	-0.016	-0.02	-0.02	-0.024
$\Delta\mu_O$	-0.032	-0.038	-0.032	-0.032	-0.032

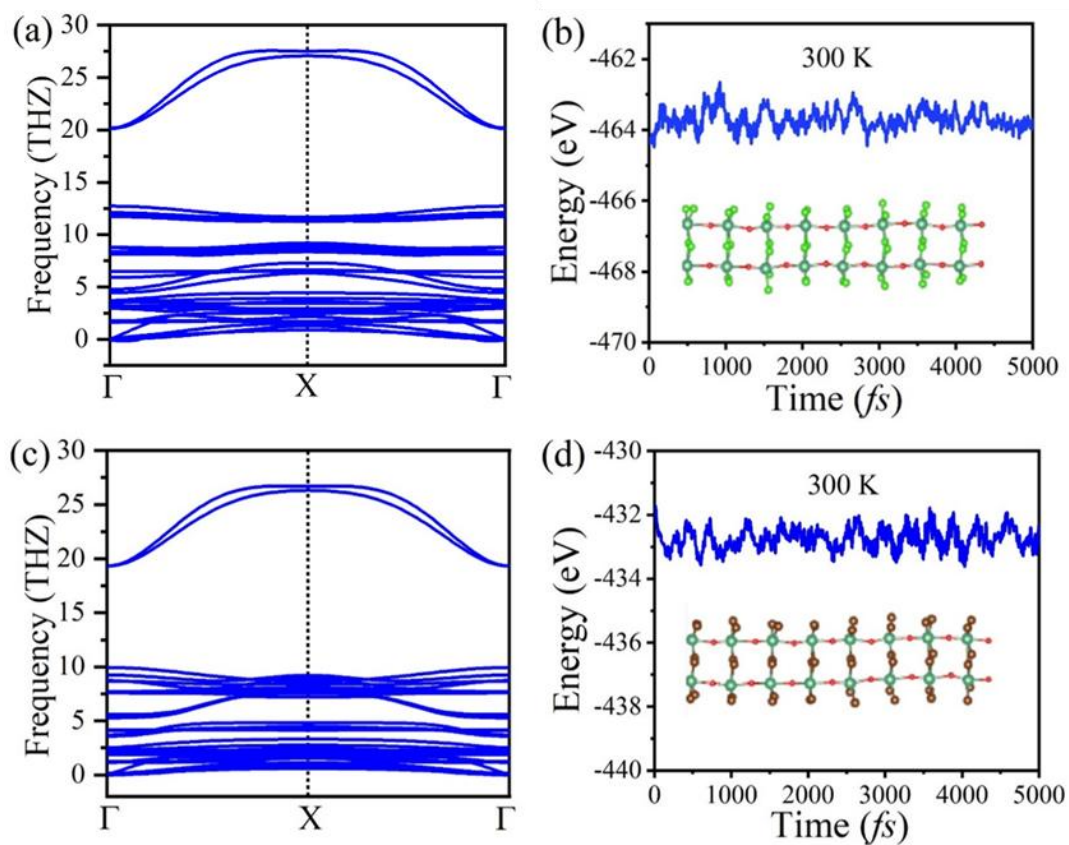


Figure S1. The phonon spectra of (a) 1D NbOCl₃ and (c) 1D NbOBr₃. The evolutions of the total energy of (b) 1D NbOCl₃ and (d) 1D NbOBr₃ with time at 300K through the AIMD simulations, and illustrations are the final atomic structures.

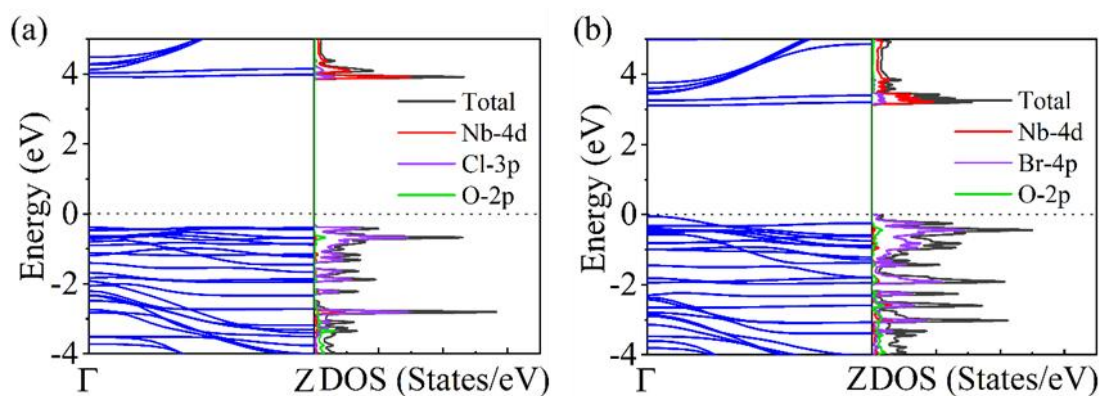


Figure S2. The band structures and projected densities of orbital states of (a) 1D NbOCl₃ and (b) 1D NbOBr₃ calculated by HSE method.

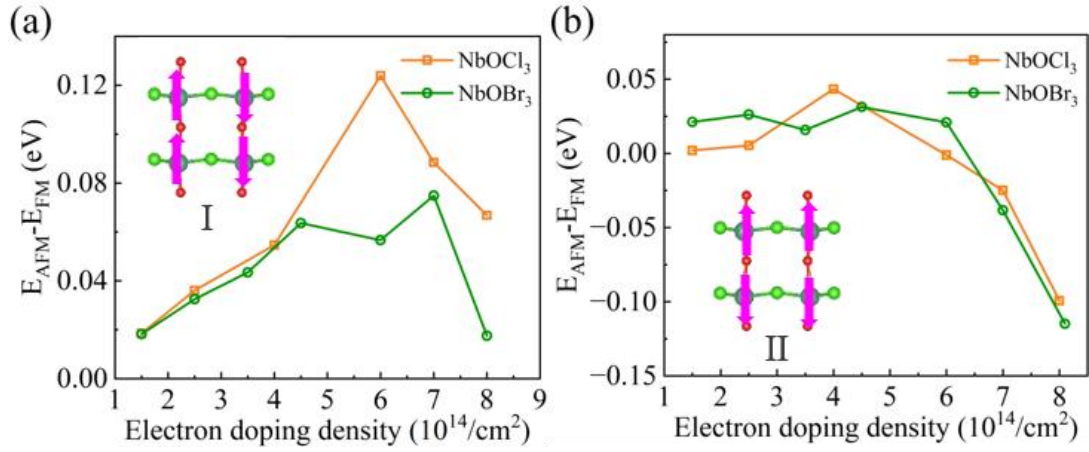


Figure S3. (a) and (b) are the energy difference of FM and two types of AFM ($\Delta E = E_{AFM} - E_{FM}$) as a function of the electron-doping concentration in 1D NbOX₃ (X=Cl, Br), the illustrations are the corresponding schematic diagrams of two types of antiferromagnetic orders.

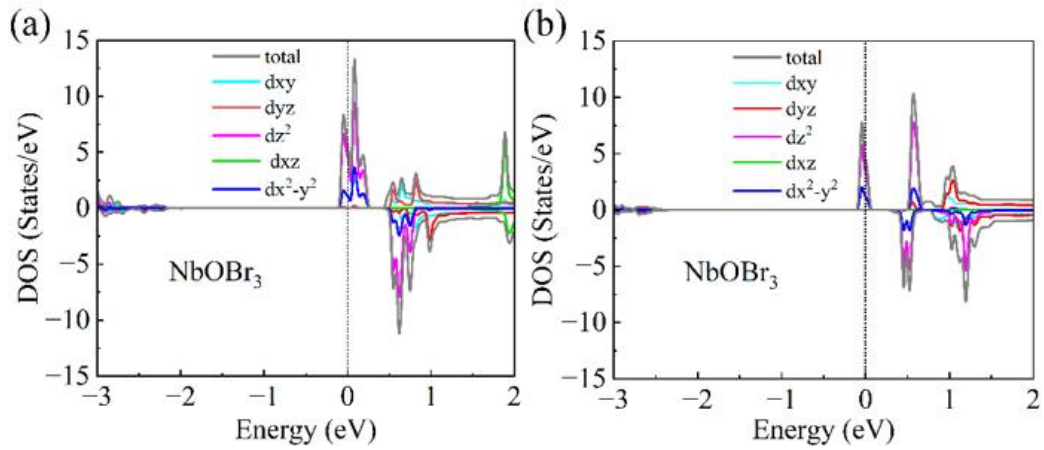


Figure S4. The PDOS of Nb-d orbital for (a) 1D NbOCl₃ at the concentration of $4.0 \times 10^{14}/\text{cm}^2$ and (b) 1D NbOBr₃ at the concentration of $3.9 \times 10^{14}/\text{cm}^2$.

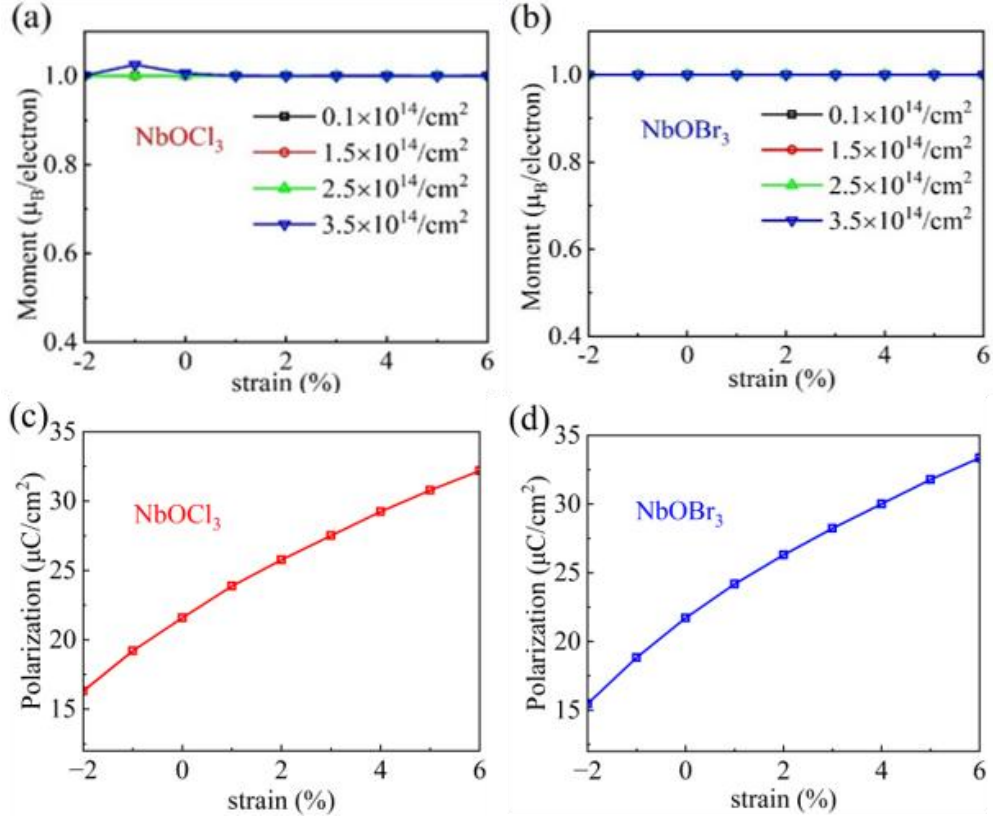


Figure S5. The doping-induced magnetic moment vs strain in (a) 1D NbOCl_3 and (b) 1D NbOBr_3 at different doping-electrons concentrations. The ferroelectric polarization under different strains without doping in (c) 1D NbOCl_3 and (d) 1D NbOBr_3 .

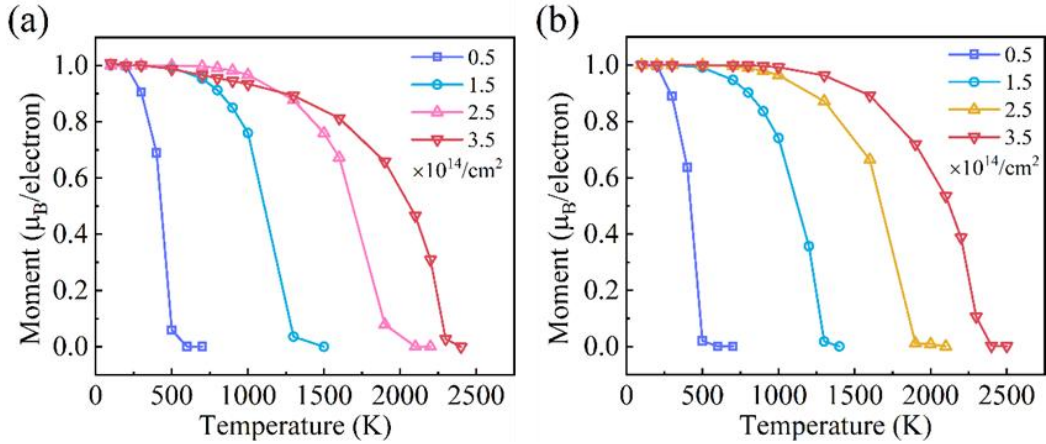


Figure S6. The spin magnetic moment vs temperature for (a) 1D NbOCl_3 and (b) 1D NbOBr_3 at different doping concentrations. In this simulation, the magnetic carriers are approximated to satisfy the Fermi-Dirac distribution function $f\left(\frac{\varepsilon-\mu}{\sigma}\right) = \frac{1}{\exp\left(\frac{\varepsilon-\mu}{\sigma}\right)+1}$, where μ is the chemical potential, and $\sigma = \kappa_B T$ is the energy broadening factor that introduces temperature effect.

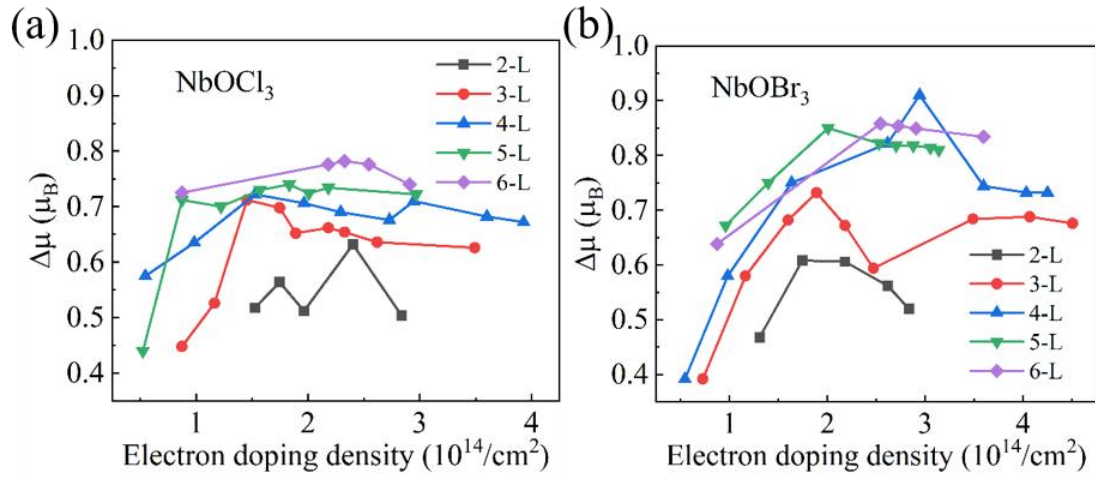


Figure S7. The magnetic moment difference ($\Delta\mu = \mu_{top} - \mu_{bot}$) of (a) n-L NbOCl_3 and (b) n-L NbOBr_3 nanochains under different doping concentrations.

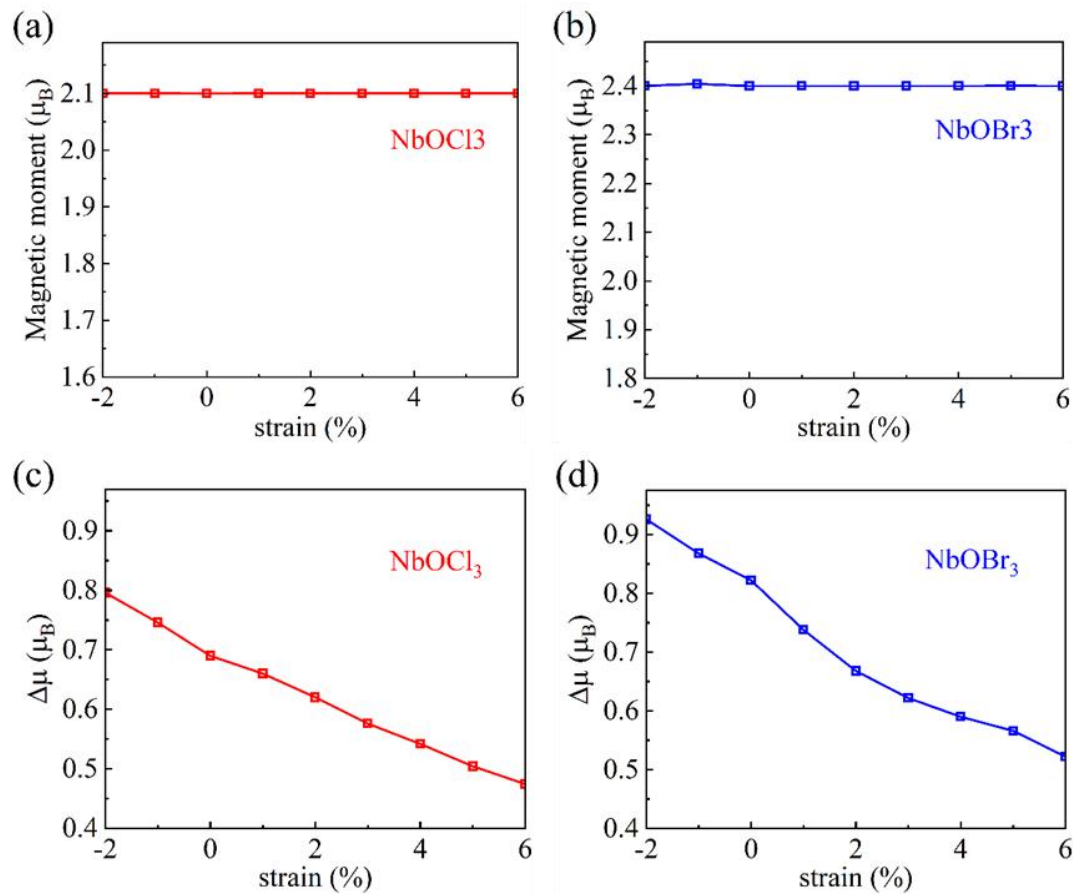


Figure S8. Under different strains, (a) the total magnetic moments and (b) magnetic moment differences of 4-L NbOCl_3 at the concentration of $2.29 \times 10^{14}/\text{cm}^2$ (doping about 2.1 electrons), (a) the total magnetic moments and (b) magnetic moment differences of 4-L NbOBr_3 at the concentration of $2.62 \times 10^{14}/\text{cm}^2$ (doping about 2.4 electrons).